Enhanced electrochemical performance of ordered mesoporous carbons by a one-step carbonization/activation treatment

Gaoxin Lin, Fan Wang, Yiliang Wang, Huaqing Xuan, Rili Yao, Zhangmin Hong, Xiaoping Dong *

Department of Chemistry, School of Sciences, Zhejiang Sci-Tech University, 928 Second Avenue, Xiasha Higher Education Zone, Hangzhou 310018, China

ARTICLE INFO

ABSTRACT

Activated ordered mesoporous carbon (AOMC) material was prepared by a one-step carbonization/activation method using SBA-15 as hard template, furfuryl alchohol (FA) as carbon source and $ZnCl_2$ as activation agent. The as-synthesized AOMC possesses hierarchical micro/mesoporous structure and high BET surface area (up to 1465.7 $m^2 \, g^{-1}$), which accelerate the ion-transport and charge-transfer during charging/discharging process for supercapacitors. A maximum specific capacitance value of 270 F g^{-1} for AOMC electrode at a current density of 1 A g^{-1} in 6 M KOH aqueous solution was obtained from the charge–discharge curves. Meanwhile, it also exhibited outstanding rate performance (~80% capacity retention from 0.5 A g^{-1} to 20 A g^{-1}) and excellent cycling stability (~94% retention after 5000 continuous charge–discharge cycles). The assembled AOMC-based symmetric cell delivers a maximum energy density of 11.8 Wh kg^{-1} at a power density of 450.1 W kg^{-1} under a voltage range of 0–1.8 V in 0.5 M Na_2SO_4 aqueous electrolyte.

1. Introduction

Supercapacitors, based on an electrical double-layer (EDL) theory, have been considered as promising electrochemical energy sources due to their high power densities, fast charge or discharge rates, and exceptionally long cycle-life[1–6]. Currently, most of electrode materials for EDL supercapacitors (EDLC) are porous carbonaceous materials because of their large surface area and plentiful porosity[7–10]. As the most used porous carbon in practical applications, commercial activated carbons suffer limitations in supercapacitors for the confined ion-diffusion in small micropores[11,12]. It has been demonstrated that mesoporous channels of 2–8 nm can accelerate the kinetic process of electrolyte transport in the electrodes[13,14].

Recently, ordered mesoporous carbon (OMC) materials have attracted numerous attentions in varied applications for their structural advantages[15–20]. As for supercapacitor application, large surface area of OMC is beneficial for the EDL formation, the carbonaceous framework hastens the electron transport and mesoporous channels improve the electrolyte diffusion. Consequently, enhanced electrochemical performance has been achieved based on OMC materials[21–23]. Whereas, compared with microporous activated carbons, OMC materials lack advantage in specific surface area. Regardless of OMC materials obtained from soft-template or hard-template strategies, their specific surface areas are limited in ~1000 $m^2 \, g^{-1}$, which is much lower than those of activated porous carbons[24–28]. For example, B. Chang et al. activated glocuse-base carbon spheres using $ZnCl_2$ and achieved porous carbon spheres with extremely high surface area of ~3000 $m^2 \, g^{-1}$[26]. Y. Wang et al. employed the same strategy to activate resorcinolformaldehyde resin spheres and gained a 2500 $m^2 \, g^{-1}$ BET surface area[27]. W. Qiao et al. used KOH to activate needle coke to develop activated carbon, whose specific surface was up to 2450 $m^2 \, g^{-1}$[28].

To further enhance the capacitance behavior, modification strategies have been performed on OMC[29–31]. One effective route is to combine OMC with pseudocapacitance materials, such as MnO_2, NiO, CoO and so on[32–35]. The hybridization of EDLC and pseudocapacitance active materials do not only overcome the relatively low capacitance, but also avert the unfavorable long-cycling stability. Another strategy for improving OMC electrochemical performance is to further activate OMC materials to obtain hierarchical porous structure with enhanced specific surface area[31,36,37]. For instance, Y. Lv et al. synthesized a kind of micro mesoporous carbon activated from KOH with the surface area of ~1400 $m^2 \, g^{-1}$ and specific capacity of 200 F g^{-1}[31]. X. Ma et al. also reported a micro/mesoporous carbon used NaOH as activation agent, which exhibited a 1600 $m^2 \, g^{-1}$ surface area and an extremely high specific capacity of 314 F g^{-1}[36]. However, these activation methods involving multi-step synthetic process are much complicated and time-consuming.

Herein, we reported a one-step carbonization/activation route to prepare activated ordered mesoporous carbon (AOMC). In comparison with non-activated OMC, these AOMC materials exhibited much larger surface area and large pore volume, developed hierarchical micro/mesoporous structure and all of these bring about the enhanced electrochemical performance for supercapacitors.

---

* Corresponding author.
  E-mail address: xpdong@zstu.edu.cn (X. Dong).

2. Experimental section

2.1. Material preparation

AOMC materials were prepared by a nanocasting route using mesoporous silica SBA-15 as a hard template. Typically, 1.0 g SBA-15 was immersed into a 20 mL ethanol solution containing 1.5 mL FA as carbon resource and 0.1 g ethanedioic acid as catalyst. After evaporating ethanol and polymerizing FA at 70 °C, the unpolymerized FA was volatilized at 150 °C. Then, 1.5 g $ZnCl_2$ as activation agent was loaded into the mixture by an impregnation method. The mixture was afterword heated in the tube furnace under a nitrogen flow at 800 °C for 2 h with a heating rate of 3 °C min^{-1}. After being cooled to room temperature, the hard template and the formed ZnO were removed by the NaOH (2 M) etching at 90 °C. The finally obtained samples were donated as AOMC.

2.2. Characterization

The X-ray diffraction (XRD) patterns of powder samples were taken by a Bruker D8 Advance diffractometer using Cu Kα radiation ($\lambda = 0.15418$ nm) as an X-ray source. Nitrogen adsorption–desorption isotherm measurements were performed at −196 °C using a micromeritics ASAP 2020 surface area analyzer. Before adsorption, the samples were out-gassed under vacuum at 150 °C for 6 h. The specific surface area (S_{BET}) was evaluated using the Brunauer–Emmett–Teller (BET) method, and the total pore volume (V_{total}) was calculated using single point method at relative pressure (P/P_0) = 0.976. And the pore size distributions were estimated according to the density functional theory (DFT) method. The morphology of the samples was observed by scanning electron microscope (SEM, Hitachi S-4800) and JEOL JEM-2100 transmission electron microscope (TEM) with an accelerating voltage of 200 KV.

2.3. Electrochemical tests

The electrochemical performance including cyclic voltammetry (CV) and galvanostatic charge/discharge (GCD) was measured by an electrochemical workstation, CHI660B (Chenhua, Shanghai, China) in a 6 M KOH aqueous solution at room temperature. In a three-electrode system, Ag/AgCl was served as the reference electrode and platinum as the counter electrode. The working electrode was made by mixing active materials, acetylene black and polyvinylidene fluoride (PVDF) with a mass ratio of 75:10:15 in a small amount of ethanol and stirred to be a paste. Then the slurry was covered on Ni foam (1 cm × 1 cm) repeatedly and dried at 100 °C for 6 h before being pressed together. In the two-electrode system, the symmetric capacitor consists of two nearly identical working electrodes using a cellulose acetate membrane as separator. Electrochemical impedance spectroscopy (EIS) was estimated in open circuit voltage with an alternate current of 5 mV in a frequency range of 0.01 HZ to 10,000 HZ.

3. Results and discussion

3.1. Microstructure characterization of AOMC

Fig. 1 shows low-angle XRD patterns of SBA-15, OMC and AOMC. Three characteristic diffractions of (100), (110) and (200) in SBA-15 pattern are corresponding to the hexagonal mesoporous structure, which is completely retained in the carbon replica of OMC. With regard to AOMC, only (100) peak is observed that does not indicate the collapse of pore structure. The intensity decrease of (100) and the disappearance of (110) and (200) can be ascribed to the etching effect of carbon pore walls.

The morphologic and structural replication of AOMC from SBA-15 is well demonstrated by SEM and TEM examinations. Fig. 2a displays a so-called worm-like morphology of SBA-15 sample that consists of
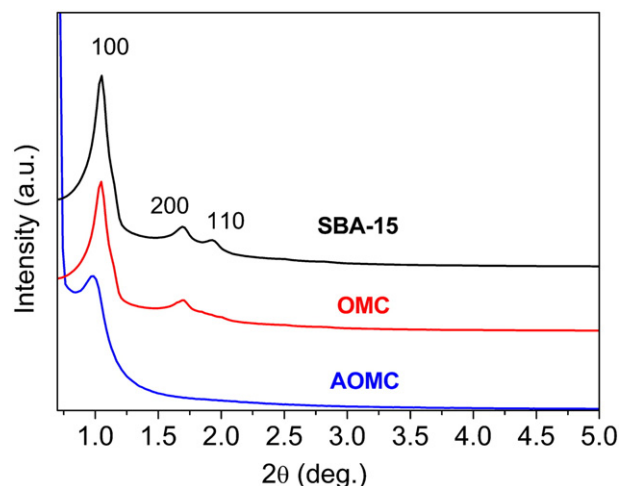

Fig. 1. XRD patterns of SBA-15, OMC and AOMC.

numerous nanorods, which is in accordance with those published literatures[38,39]. The replicated sample OMC by SBA-15 well inherits the nanorod shape as seen in Fig. 2b. As exhibited in Fig. 2c, the SEM image of AOMC depicts a rod-like aspect that is similar to SBA-15 and OMC. Such morphology is also demonstrated by the TEM image (Fig. 3c). The TEM image of SBA-15 (Fig. 3a) illustrates a highly ordered hexagonal pore structure that is completely retained in OMC and AOMC samples. It is noticeable that the relative size of pore wall and pore channel is reversal in OMC sample, which suggests the successful nanocasting process. In comparison with OMC, its pore size is apparently enhanced because of the activation effect of $ZnCl_2$. Moreover, the perfect retention of ordered pore structure in AOMC indicates that the decrease in intensity and the disappearance of diffractions in XRD pattern are not ascribed to the breakdown of pore structure.

Fig. 4 presents the nitrogen sorption isotherms and the corresponding pore size distributions of OMC and AOMC. Two samples show type IV isotherms with a marked leap at medium pressure range, which is a characteristic for mesoporous structure. Obviously, two isotherms have the characteristic H2 hysteresis loop, demonstrating a kind of ink bottle type pores[40]. And the hysteresis loop of AOMC shifts to higher relative pressure compared with OMC, suggesting the enlargement of pore size (Fig. 4a). Fig. 4b shows the pore size distribution of OMC and AOMC, where the narrow distribution of OMC centers at 4.8 nm. After activation, the pore size distribution of AOMC broadens and the peak center is enlarged to 8.7 nm. Pore structure parameters of OMC and AOMC materials are listed in Table 1. In contrast with the non-activated sample of OMC, AOMC sample exhibits enhanced BET surface area that results from the microporous and secondary mesoporous structure produced by the chemical activation. The sample of AOMC possesses a high BET surface area of 1465.7 $m^2 g^{-1}$ and a large pore volume of 1.6 $cm^3 g^{-1}$, as well as a superior hierarchical micro/mesoporous structure.

3.2. Electrochemical performance of AOMC in three-electrode system

Such superior porous structure endues AOMC with excellent electrochemical performance. As shown in Fig. 5a, similar quasi rectangular shape is found in these cyclic voltammetry (CV) curves of AOMC with various scan rates in 6 M KOH electrolyte, which manifests the approximately ideal EDLC behavior and the high rate capability[29,30]. And when the scan rate reaches 100 mV s^{-1}, the curve shows a little distorted shape which should be ascribed to the reasons as follows: (1) the oxidation of carbon contributes an additional pseudocapacitance